

# Software Verification For System Level Implementation Of Cylindrical Dielectric Resonator Antenna For High Speed Real-Time Applications

Anshu Thakur

Dept. of Electronics & Comm. Engineering  
Aravali College of Engineering & Management  
Faridabad, Haryana, India

Dr. S. V. A. V. Prasad

Dean, Dept. of R&D and Industrial Consultancy  
Lingaya's University  
Faridabad, Haryana, India

**Abstract**—With the advancements in the field of communication technology, it has been seen that many different architectures and configurations of antenna have emerged. One of the most popular type of antenna is the Dielectric Resonator Antenna (DRA) which has been quite prominent in most modern high speed communication applications. Although, the design of DRA in various geometric forms have already been accomplished, the methodology for the design which is followed is not at all systematic. In this paper, elaborate software based verification of a system level implementation for cylindrical DRA has been achieved with an aim to demonstrate the feasibility of such an approach in conjunction with the mathematical framework for systematic design of DRA.

**Keywords**—Dielectric Resonator Antenna (DRA); MATLAB; Iterative Design; Mathematical Modeling; System Level Design (SLD)

## I. INTRODUCTION

Since about 1970's, dielectric resonators have helped achieve the miniaturization of active and passive microwave components, such as oscillators and filters [1, 2] and have proved to be one of the driving forces behind advancement of communication systems such as Spatial Division Multiple Access.

In a shielded environment, the resonators built with DRs can reach the unloaded Q factor of 20,000 at frequencies between 2 and 20 GHz. The principle of operation of the dielectric resonator can best be understood by studying the propagation of electromagnetic waves on a dielectric rod waveguide. The mathematical description and the experimental verification of the existence of these waves have been known for a long time. Their massive application, however, began with the introduction of optical fibers.

Consider the lowest modes of propagation on dielectric rod waveguides as shown in Figures 1-3 [3]. The first index denotes the number of full-period field

variations in azimuthal direction, and the second one the number of radial variations.

When the first index is equal to zero, the electromagnetic field is circularly symmetric. In the cross sectional view, the field lines can be either concentric circles (e.g. the E field of the  $TE_{01}$  mode), or the radial straight line (e.g. the H field of the same mode). For higher modes, the pure transverse electric or transverse magnetic fields cannot exist, so that both electric and magnetic fields must have non-vanishing longitudinal components. Such modes are called hybrid electromagnetic (HEM), the lowest of them being HEM<sub>11</sub>. The fields are properly expressed in terms of Bessel functions, and there exist closed form expressions for determining the wavelength and the propagation velocity of these waves.

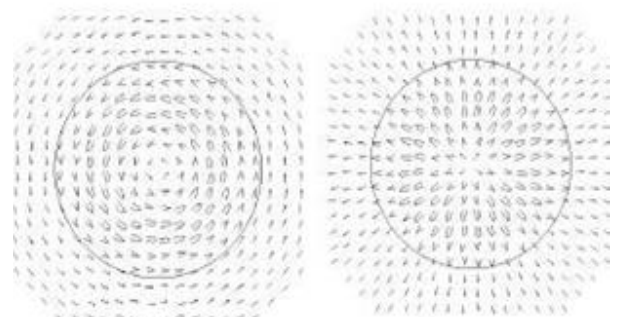


Fig. 1: Mode  $TE_{01}$  on a dielectric rod waveguide. Left figure shows E-field while Right figure shows H-field

When only a truncated section of the dielectric rod waveguide is used, one obtains a resonant cavity in which the standing waves appear. Such a device is called dielectric resonator. When a dielectric resonator is not entirely enclosed by a conductive boundary, it can radiate, and so it becomes an antenna. DR antenna was successfully built and described in [4], while the rigorous numerical solution was published in [5]. Review treatments of DR antennas can be found in [6], [7] and [8].

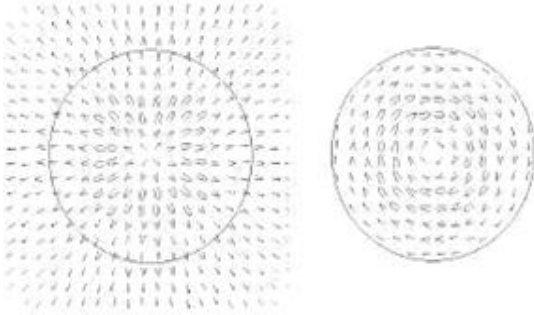
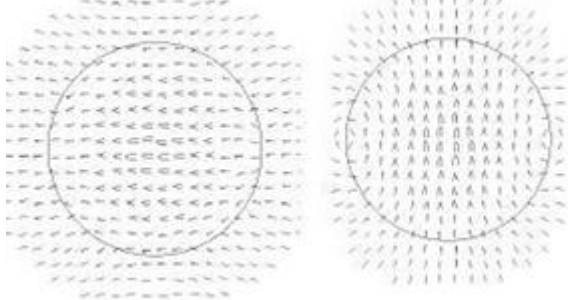


Fig. 2: Mode  $TM_{01}$  on a dielectric rod waveguide. Left figure shows E-field while Right figure shows H-



field

Fig. 3: Mode  $HEM_{11}$  on a dielectric rod waveguide. Left figure shows E-field while Right figure shows H-field

The numerical investigation of the DRA was started as an attempt to determine the natural frequencies of various modes of an isolated dielectric resonator, without any other scattering object in its vicinity, and without any excitation mechanism. It was found that the resonant frequencies were complex valued:

$$s_{m,n} = \sigma_{m,n} + j\omega_{m,n} \quad (1)$$

Each particular solution corresponds to a resonant  $m, n$  type mode that satisfies all the boundary and continuity conditions. For rotationally symmetric resonators, subscript  $m$  denotes the number of azimuthal variations, and subscript  $n$  denotes the order of appearance of modes in the growing frequency direction.

The resonant frequency has a non-vanishing real part which signifies that such a mode would oscillate in an exponentially decaying manner, if it were initially excited by an abrupt external stimulus. The ratio of the real to the imaginary part of the natural frequency is the radiation Q factor of the mode given as:

$$Q_r = -\frac{\omega_{m,n}}{2\sigma_{m,n}} \quad (2)$$

For given dimensions and dielectric constant, numerical solution can determine the resonant frequency and the radiation Q factor. Such computed data can then be fitted to some convenient analytic expressions [9]. In this work, we proceed to find such analytic expressions which can closely simulate the actual behavior of a dielectric resonator antenna and hence can be used for real-time communication

systems which are highly sensitive to various antenna parameters.

## II. CYLINDRICAL DIELECTRIC RESONATOR

The general coordinate system used for the study and analysis of the cylindrical DRA in this work is shown in Fig. 4. This coordinate system is fairly general in the sense that it finds its use in study and analysis of electromagnetic field theory in cylindrical coordinate systems.

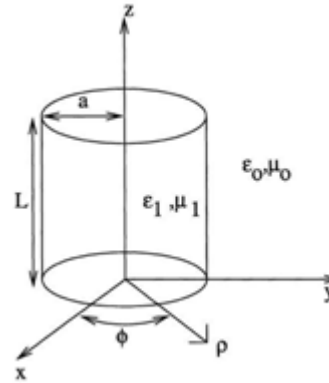


Fig. 4: General Coordinate System for Cylindrical DRA

Cylindrical DRAs are usually placed on a ground plane and is excited using a probe or aperture. It usually has an aspect ratio of about 0.5 to 4. The radiation pattern and the feeding method depend on the mode of interest. The DRA can resonate at many different modes. For the cylindrical DRA, the modes are analysed and indexed in a similar manner as the dielectric waveguide.

As is the case with dielectric waveguides, to satisfy the boundary conditions of continuity of tangential fields at the boundary of the dielectric and air, the only transverse fields that can exist are the modes with no azimuthal variation. All the other modes are hybrid modes.

A lot of conventional feeding mechanisms for DRA have been studied which are mostly derived from the theory of feeding structures for waveguides and cavities. In practice, it is typical to see DRAs being excited by a short monopole antenna or half circular current loops.

Another important aspect of the analysis of DRA is the radiation pattern. Fundamental modes of DRA radiate like magnetic or electric dipoles because of the fact that field distributions in the cavity for the low order modes support these terms. To study the radiation pattern, a nice approach is to expand the radiated fields using the multipole expansion technique which involves the decomposition of any arbitrary radiation pattern into a sum of dipole, quadrupole and higher order multiple pole terms.

For low profile antennas operated at low order modes, the contributions of the higher order poles are weak. Generally, the smaller the radiating element is compared to the free space wavelength, the better

this approximation is. The radiation pattern as a function of elevation angle for a typical circular DRA with two modes excited in quadrature phase is shown in Fig. 5.

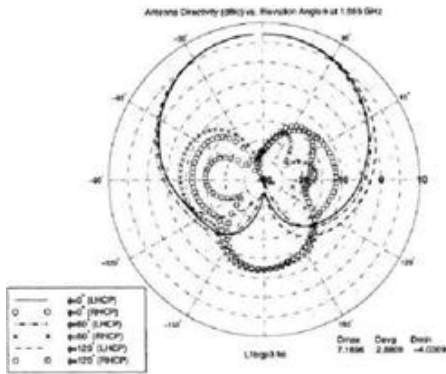


Fig. 5: Radiation Pattern as a function of elevation angle for circular DRA

The approximate field distributions inside the cylinder for the first three common modes are shown below:

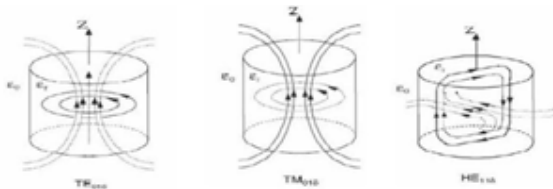


Fig. 6: Field distributions inside a cylindrical DRA

The far field radiation patterns for the TE01 modes are shown below, the second figure being the 3D equivalent of the first figure. It is clear that the electric field is doughnut-shaped.

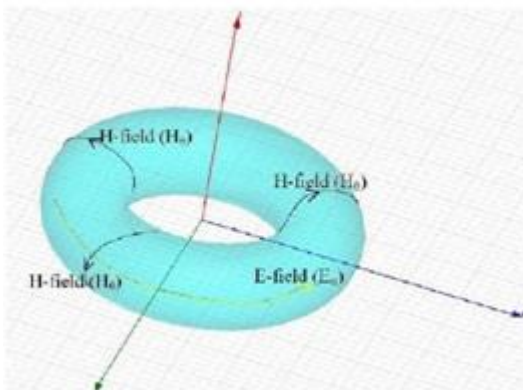
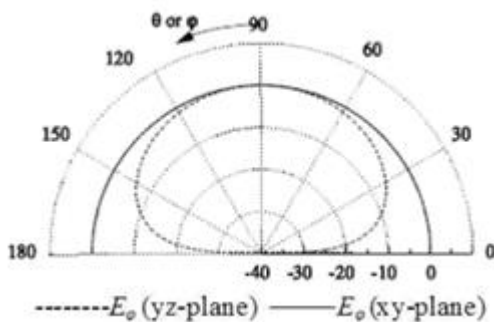


Fig. 7: Far-field radiation pattern for TE<sub>01</sub> mode

The far field radiation patterns for the TM<sub>01</sub> modes are shown below.

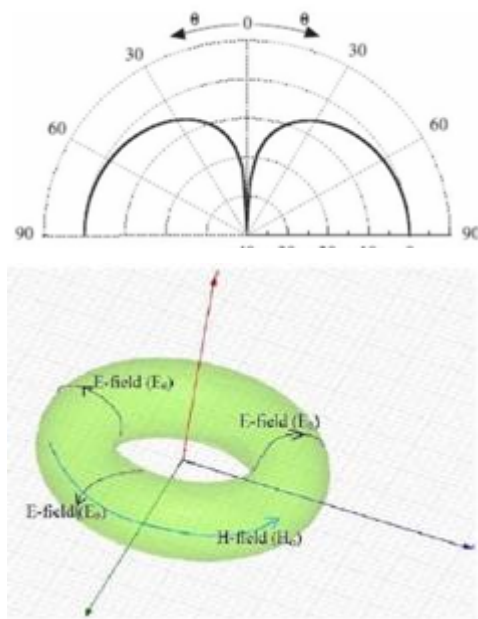


Fig. 8: Far field radiation pattern for TM<sub>01</sub> mode

Clearly, the radiation pattern of the TM<sub>01</sub> mode looks like a z-directed half-wavelength electric dipole and the TE<sub>01</sub> mode looks like a z-directed half-wavelength magnetic dipole. These kinds of insights are actually very useful towards building a mathematical model from existing mathematical frameworks.

The radiation pattern of the HE<sub>11</sub> mode resembles the radiation pattern of a half-wavelength electric dipole along the y axis and is shown in Fig. 9.

### III. SYSTEM LEVEL IMPLEMENTATION OF THE DRA

To demonstrate the suitability of the mathematical approach as elucidated here, the authors of the paper accomplished a system level implementation of a cylindrical DRA for high speed communication system applications.

Various parametric characteristics of the DRA are as follows :-

Parameter	Value
Height	10.5 microns
Radius	1.5 microns
Co-axial feed line	9 microns
Permittivity	31.5

Based on the above parameters, the graphical representation of the cylindrical DRA can be shown as

per Fig. 10. The DRA is usually operated at one of its lower order modes. At its lower order modes, the field lines show a behavior very similar to the lower order terms of the multipole expansion. Therefore, the radiation pattern is expected to show a radiation pattern that is similar to the corresponding multipole term.

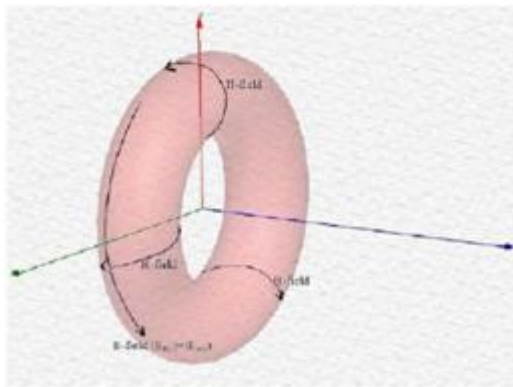
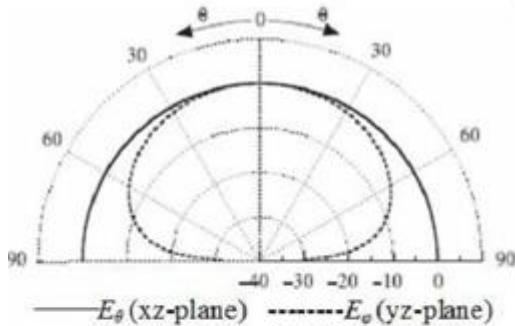


Fig. 9: Far field radiation pattern for  $HE_{11}$  mode

Thus, the DRA is like a tiny aperture sitting in free space that radiates energy away. This view of the circular DRA eases away most of the non-linear behavior due to local perturbations and only leaves terms which essentially capture the local dynamics of the DRA whose understanding is essential.

The DRA has been fabricated in lab and has been tested with the help of microwave test bench. However, before the fabrication of the DRA could be realized, there were several challenges that was needed to be mitigated. One of the inherited advantages of DRA is its use at millimetre wave frequencies and until a very sophisticated process aided by micromachining is available a poor fabrication process is involved.

Fabrication of the DRA has been achieved by using a copper plate as the background plane and then attaching the Dielectric Resonator on the ground plane through an adhesive with very tiny dielectric permittivity as compared to the DRA. The process of etching was used to bond the DRA onto the copper plane with adhesive to fully secure the antenna and later enclosed in a plastic case that does not alter the radiating capabilities of the antenna.

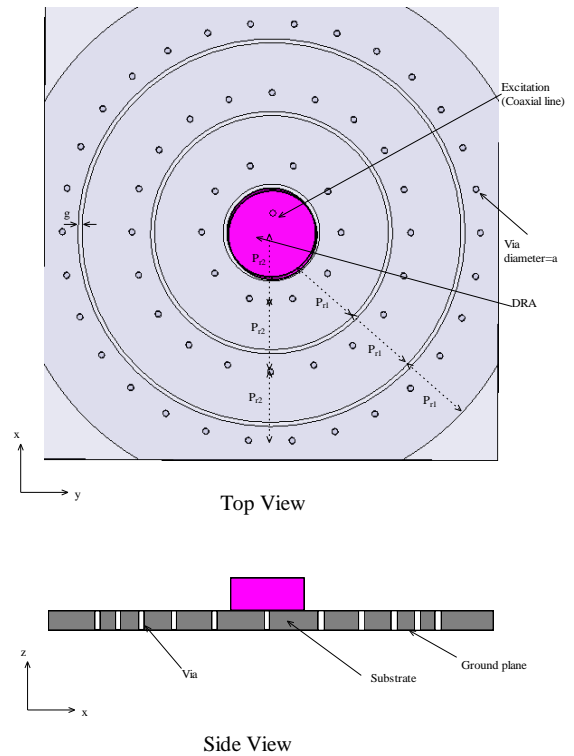


Fig. 10: Graphical representation of DRA design

The choice of specific adhesive and plastic enclosure also plays a very important role. If adhesive with very high permittivity is chosen, then it can substantially alter the properties of the DRA and hinder its performance. Ideally, the permittivity of the adhesive must be very very small as compared to the dielectric resonator such that it can be neglected. If it is comparable to that of the dielectric resonator, then the system acts like a segmented DRA and the liquid adhesive heats up and alters its chemical properties which can substantially affect the properties of the dielectric resonator also.

The radiation pattern of the proposed circular DRA has been obtained from both theoretical simulation using HFSS tool from ANSYS and also practical observation in the lab using microwave testbench. The radiation pattern shows that the circular DRA is capable of performing well even in the absence of Etched Background Plane. Although, the radiation pattern with Etched Background Plane is better and shows more directivity. The plot of the radiation pattern can be seen in Fig. 11.

Various other associated operational parameters of the DRA were also observed in the microwave lab using the testbench and exciting the antenna using Klystron tube. The various parameters are relevant for the system designer to know before he can use it for communication purposes. These operational parameters and their values often form part of the datasheet of an antenna which is always supplied when one buys it as a standalone device. These operational parameters for the circular DRA are as follows :

Operational Parameters	Value
Beamwidth	72/60
VSWR	< 1.5
Impedance	50 Ohms
Operational Parameters	Value
Polarization	Vertical
Max Power	45 W
Frequency Range	1.75 – 4.5 GHz

These operational parameters were ascertained in the microwave lab using microwave test bench and by conducting series of tests to remove any ambiguity and tolerance factors. The above values are exact as measured in the tests and has an average tolerance or variation factor of around 0.5%. Such precise and accurate manufacturing of DRA is necessary for industrial deployment where the environment is such that precision and accuracy plays a very important role in the commercial success of the project.

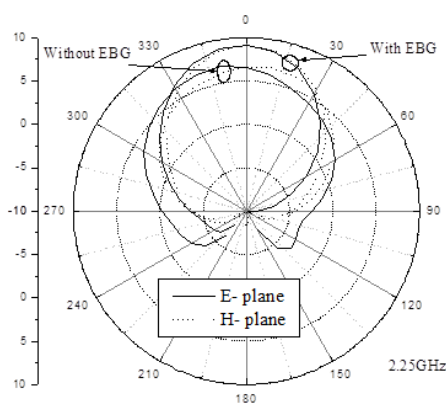


Fig. 11: Radiation Pattern of the DRA

#### IV. SOFTWARE VERIFICATION

The proposed DRA was used to design a fully working transmitter/receiver pair after the fabrication of the antenna, as it was embedded on an electronic system namely IEEE 802.11 wireless 4G LTE transceiver to test its efficiency and operational characteristics. Initially, MATLAB based system level design was created to obtain theoretical results based on simulation. This system level design was accomplished by creating a block diagram in Simulink with blocks taken from Communication Systems Toolbox.

These blocks when joined together formed a system whose performance could be simulated using a discrete time event driven simulation paradigm. This paradigm basically depends on solving the system of difference equations which is automatically deduced by MATLAB/Simulink Compiler. After solving the equations, the roots are assigned an initial time stamp of  $t = 0$  and then iterated over regular intervals to plot necessary graphs and performance variables.

This approach is very powerful for software based prototyping before an actual hardware is created to reduce time, efforts and most importantly money. Modern engineering has come to a point where extremely complex systems are required to be designed in very short time. Getting the manufacturing and fabrication right the first time is paramount for project success. Under such circumstances software based validation is sought where the engineers can feel assured about the system performance and accuracy through software simulation before it is manufactured and tested in practice. This has been embraced in this research work also keeping it relevant to industry standards.

After the design and simulation of the hardware in MATLAB, the theoretical simulated result was compared with actual hardware result through hardware software co-simulation. The figure in the next page shows the MATLAB implementation of the LTE system embedded with our proposed DRA. This system basically shows how the MIMO OFDM transmitter and receiver operate in accordance with IEEE 802.11 specifications with QAM modulation to deliver the communication packets in high speed.

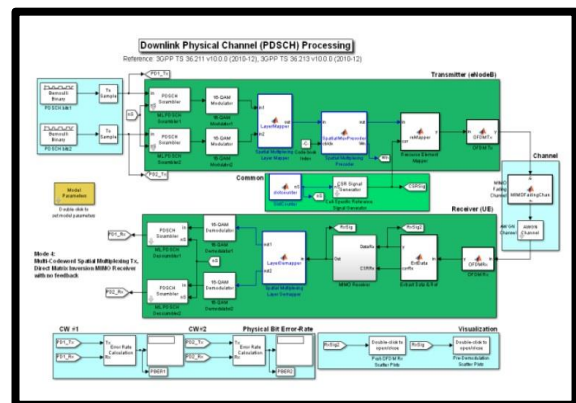


Fig. 12: MATLAB/Simulink based System Implementation

The primary motivation for use of OFDM in a specified MIMO channel is due to the fact that OFDM modulation converts a frequency-selective MIMO channel into an equivalent set of parallel MIMO channels which are frequency-flat. This makes the equalization of multi-channel signals particularly simple, since now for each OFDM-tone there is only a constant matrix which must be inverted.

There are basically N subcarriers (or tones) in a typical MIMO-OFDM system, and the individual distinct streams of data are passed through the OFDM

modulators first which perform an IFFT which is the Inverse Fast Fourier Transform on the given blocks having length  $N$  and subsequently followed by a parallel-to-serial conversion. After this, cyclic prefix (CP) of length  $L_{cp} \geq L$  which contains a copy of the last samples of  $L_{cp}$  of the output of the parallel-to-serial conversion of the  $N$ -point IFFT is further prepended.

These OFDM symbols which have resulted and have length of  $N + L_{cp}$  are transmitted simultaneously from the individual antennas. In the receiver end, these individual signals are first passed through what are known as OFDM demodulators where the CP is discarded first and then an  $N$ -point FFT or Fast Fourier Transform is performed on the sequence. The outputs coming from the OFDM demodulators are then finally separated and ultimately decoded to reveal the information. In the above system design, the spectral efficiency loss is completely ignored owing to the presence of the CP as it only contains redundant information.

It is assumed that the channel used for communication is purely Rayleigh fading channel, ergodic and remains constant over the block which spans at least one symbol of OFDM and subsequently changes in an independent fashion from one block to another. For simplicity's sake, attention is primarily restricted to the case of receiver correlation only.

This system can operate with reduced latency bounds by using proposed circular DRA. Through this system, it would be possible to simulate and verify the operational limits of the circular DRA in a real-time setting of a full-fledged communication system. This LTE system upon simulation yields two primary parameters viz. BER curve and FFT spectrum.

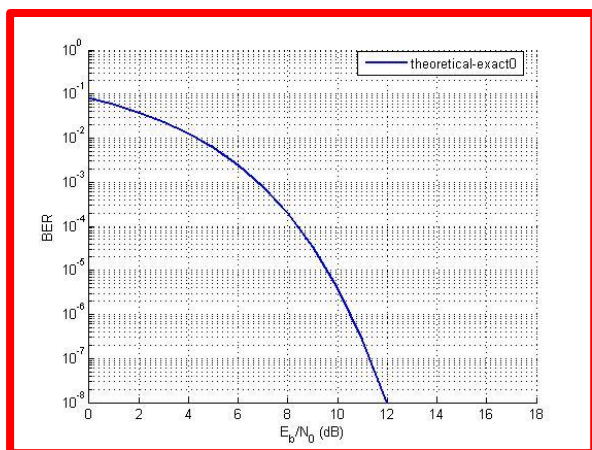


Fig. 13: Simulated BER Curve of the System

The curve shows optimal performance of the system with low BER. Lower the Bit Error Rate of the communication system, higher is the efficiency of the communication system and this has been possible only because of the higher operational tolerance and performance of the circular DRA. Without the circular DRA, it would have been impossible for the system to achieve this BER curve in the absence of any error

correction and detection schemes in the transmitter and receiver. Hence, the cylindrical DRA not only transmits and receives the data accurately but also manages to do so with high efficiency owing to reduced surface waves, low return loss, high gain and specifically high directivity of the beam.

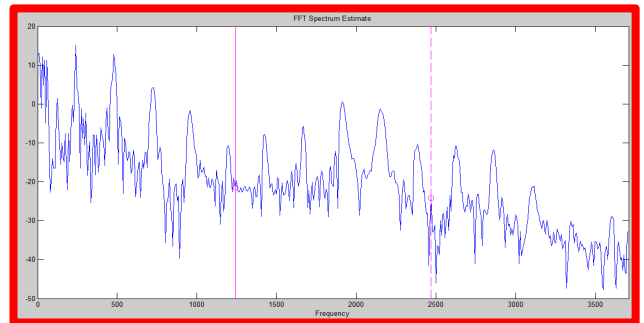


Fig. 14: Simulated FFT Spectrum of the System

The simulated FFT spectrum of the system is also shown here. The FFT spectrum of the hardware shows that the total harmonic distortion or the noise percentage is within the tolerance level as the average of all the peaks comes at approximately  $-10$  Hz which is well below the specification of  $-25$  Hz. This tells that the simulated hardware works in principle and can be fabricated as actual hardware as well to validate the circular DRA using hardware software co-simulation.

## V. CONCLUSION & FUTURE WORK

In this work, we basically analyzed various properties of a cylindrical DRA from a purely Electromagnetic Field Theory point of view and went onto show its correlation with properties that can be considered as its design features.

Using the operational characteristics, system level design of DRA based communication system employing MIMO-OFDM is achieved and its detailed simulation was carried out using MATLAB/Simulink.

The simulation showed how BER curves and FFT spectrum are optimized for real-time applications demonstrating the accuracy of the analysis and the system design.

Future avenues for taking this work forward may include using different modulation schemes and using different bands for communication employing millimeter waves and beyond for ultra-high speed communication systems.

## REFERENCES

- [1] J. K. Plourde and C. L. Ren, —Application of dielectric resonators in microwave components, IEEE Trans. Microwave Theory Techn., vol. MTT-29, no. 8, pp. 754-770, August 1981.
- [2] Dielectric Resonators, D. Kajfez and P. Guillon (eds.), Norwood, MA: Artech House, 1986.
- [3] Dielectric Resonator Antenna – Possible Candidate for Adaptive Antenna Array by D. Kajfez and Ahmed A. Kishk

[4] S. A. Long, M. McAllister and L. C. Shen, —The resonant cylindrical dielectric cavity antenna,|| IEEE Trans. Antennas Propagat., vol AP-31, pop. 406-412, May 1983.

[5] A. W. Glisson, D. Kajfez and J. James, —Evaluation of modes in dielectric resonators using a surface integral equation formulation,|| IEEE Trans. Microwave Theory Tech., vol. MTT-31, pp. 1023-1029, December 1983.

[6] R. K. Mongia and P. Bhartia, —Dielectric resonator antennas - a review and general design relations for resonant frequency and bandwidth,|| Intrenat'l Jour. Microwave and Millimeter-Wave Computer-Aided Engineering, vol. 4, no. 3, pp. 230-247, 1994.

[7] A. Petosa, D. J. Roscoe, A. Ittipibon and M. Cuhaci,—Antenna research at the communications Research Centre,|| IEEE Antennas Propag. Mag., vol. 37, no. 5, pp. 7-18, October 1996.

[8] A. Petosa, A. Ittipibon, Y. M. M. Antar, D. Roscoe and M. Cuhaci, —Recent advances in dielectric-resonator antenna technology,|| IEEE Antennas Propag. Mag., vol. 40, no. 3, pp. 35-48, June 1998.

[9] A. A. Kishk, A.W. Glisson and D. Kajfez, "Computed resonant frequency and far fields of isolated dielectric discs," IEEE Antennas and Propagation Society International Symposium Digest, vol. 1, pp. 408-411, 1993.